Increasing the Interpretability of Recurrent Neural Networks Using Hidden Markov Models

Viktoriya Krakovna VKRAKOVNA@FAS.HARVARD.EDU
Department of Statistics, Harvard University

Finale Doshi-Velez FINALE@SEAS.HARVARD.EDU
Department of Computer Science, Harvard University

Abstract

As deep neural networks continue to revolutionize various application domains, there is increasing interest in making these powerful models more understandable and interpretable, and narrowing down the causes of good and bad predictions. We focus on recurrent neural networks (RNNs), state of the art models in speech recognition and translation. Our approach to increasing interpretability is by combining an RNN with a hidden Markov model (HMM), a simpler and more transparent model. We explore various combinations of RNNs and HMMs: an HMM trained on LSTM states; a hybrid model where an HMM is trained first, then a small LSTM is given HMM state distributions and trained to fill in gaps in the HMM's performance; and a jointly trained hybrid model. We find that the LSTM and HMM learn complementary information about the features in the text.

1. Introduction

Following the recent progress in deep learning, researchers and practitioners of machine learning are recognizing the importance of understanding and interpreting what goes on inside these black box models. Recurrent neural networks have recently revolutionized speech recognition and translation, and these powerful models could be very useful in other applications involving sequential data. However, adoption has been slow in applications such as health care, where practitioners are reluctant to let an opaque expert system make crucial decisions. If we can make the inner workings of RNNs more interpretable, more applications can benefit from their power.

2016 ICML Workshop on Human Interpretability in Machine Learning (WHI 2016), New York, NY, USA.

There are several aspects of what makes a model or algorithm understandable to humans. One aspect is model complexity or parsimony. Another aspect is the ability to trace back from a prediction or model component to particularly influential features in the data (Rüping, 2006) (Kim et al., 2015). This could be useful for understanding mistakes made by neural networks, which have human-level performance most of the time, but can perform very poorly on seemingly easy cases. For instance, convolutional networks can misclassify adversarial examples with very high confidence (Nguyen et al., 2015), and made headlines in 2015 when the image tagging algorithm in Google Photos mislabeled African Americans as gorillas. It's reasonable to expect recurrent networks to fail in similar ways as well. It would thus be useful to have more visibility into where these sorts of errors come from, i.e. which groups of features contribute to such flawed predictions.

Several promising approaches to interpreting RNNs have been developed recently. Che et al. (2015) have approached this by using gradient boosting trees to predict LSTM output probabilities and explain which features played a part in the prediction. They do not model the internal structure of the LSTM, but instead approximate the entire architecture as a black box. Karpathy et al. (2016) showed that some LSTM cell states can be interpreted with the naked eye by color-coding the text data with the cell state values, and showing that some of them track quotes, brackets and other clearly identifiable aspects of the text. Building on these results, we take a somewhat more systematic approach to looking for interpretable hidden states, by using decision trees to predict individual hidden states (Figure 2). We visualize the overall dynamics of the hidden states by coloring the training data with the k-means states (Figures 3b, 3d).

We explore several approaches to building interpretable models by combining RNNs and HMMs. The existing body of literature mostly focuses on methods that specifically train the RNN to predict HMM states (Bourlard & Morgan, 1994) or posteriors (Maas et al., 2012), referred to as hybrid or tandem methods respectively. In order to model the big picture of the state changes in the LSTM, we extract the hidden states and approximate them with a continuous emission hidden Markov model (HMM). This approach does not require the RNN to be modified in order to make it understandable, as the interpretation happens after the fact. In order to build a model with fewer LSTM states, we take the reverse approach where an HMM is trained first, and the HMM state probabilities are added to the output layer of the LSTM (see Figure 1). The LSTM model can then make use of the information from the HMM, and fill in the gaps when the HMM is not performing well, resulting in an LSTM with a smaller number of components that could be interpreted individually (Figures 3, 4).

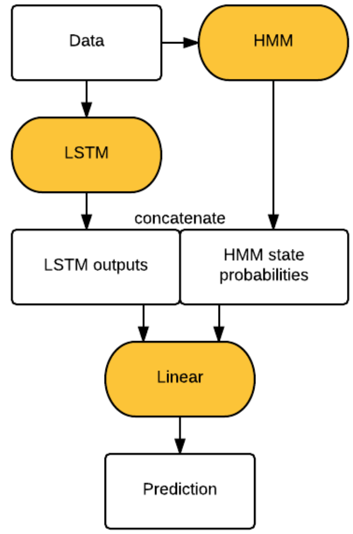

Figure 1: Hybrid HMM-LSTM algorithm.

2. Methods

We compare a hybrid HMM-LSTM approach with a continuous emission HMM (trained on LSTM states), and a discrete emission HMM (trained directly on data).

2.1. LSTM models

We use a character-level LSTM with 1 layer and no dropout, based on the Element-Research library. We train the LSTM for 10 epochs, starting with a learning rate of 1, where the learning rate is halved whenever $\exp(-l_t) > \exp(-l_{t-1}) + 1$, where l_t is the log likelihood score at epoch t. The L_2-norm of the parameter gradient vector is clipped at a threshold of 5.

2.2. Hidden Markov models

The HMM training procedure is as follows:

Initialization of HMM hidden states:

(Discrete HMM) Random multinomial draw for each time step (i.i.d. across time steps).

(Continuous HMM) K-means clusters fit on LSTM states, to speed up convergence relative to random initialization.

At each iteration:

1. Sample states using Forward Filtering Backwards Sampling algorithm (FFBS, Rao & Teh (2013)).

2. Sample transition parameters from a Multinomial-Dirichlet posterior. Let n_{ij} be the number of transitions from state i to state j. Then the posterior distribution of the i-th row of transition matrix T (corresponding to transitions from state i) is:

$$T_i \sim \text{Mult}(n_{ij}|T_i)\text{Dir}(T_i|\alpha)$$

where α is the Dirichlet hyperparameter.

3. (Continuous HMM) Sample multivariate normal emission parameters from Normal-Inverse-Wishart posterior for state i:

$$\mu_i, \Sigma_i \sim N(y|\mu_i, \Sigma_i)N(\mu_i|0, \Sigma_i)\text{IW}(\Sigma_i)$$

(Discrete HMM) Sample the emission parameters from a Multinomial-Dirichlet posterior.

Evaluation:

We evaluate the methods on how well they predict the next observation in the validation set. For the HMM models, we do a forward pass on the validation set (no backward pass unlike the full FFBS), and compute the HMM state distribution vector p_t for each time step t. Then we compute the predictive likelihood for the next observation as follows:

$$P(y_{t+1}|p_t) = \sum_{x_t=1}^{n} \sum_{x_{t+1}=1}^{n} p_{tx_t} \cdot T_{x_t,x_{t+1}} \cdot P(y_{t+1}|x_{t+1})$$

where n is the number of hidden states in the HMM.

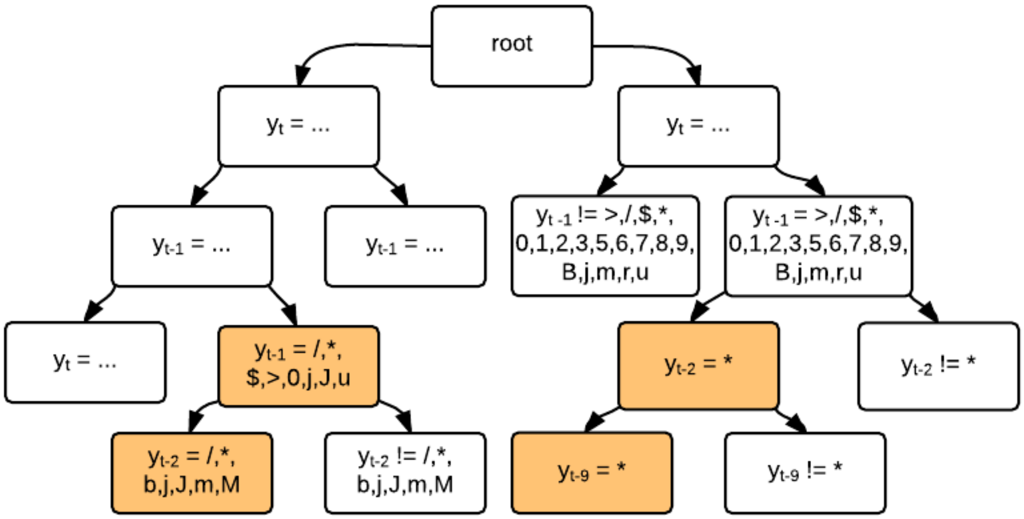

Figure 2: Decision tree predicting an individual hidden state of the hybrid algorithm based on the preceding characters on the Linux data. The hidden states of the 10-state hybrid mostly track comment characters.

2.3. Hybrid models

Our main hybrid model is put together sequentially, as shown in Figure 1. We first run the discrete HMM on the data, outputting the hidden state distributions obtained by the HMM's forward pass, and then add this information to the architecture in parallel with a 1-layer LSTM. The linear layer between the LSTM and the prediction layer is augmented with an extra column for each HMM state. The LSTM component of this architecture can be smaller than a standalone LSTM, since it only needs to fill in the gaps in the HMM's predictions. The HMM is written in Python, and the rest of the architecture is in Torch.

We also build a joint hybrid model, where the LSTM and HMM are simultaneously trained in Torch (we implemented an HMM Torch module, optimized using stochastic gradient descent rather than FFBS). Similarly to the sequential hybrid model, we concatenate the LSTM outputs with the HMM state probabilities.

3. Experiments

We test the models on several text data sets on the character level: the Penn Tree Bank (5M characters), and two data sets used by Karpathy et al. (2016), Tiny Shakespeare (1M characters) and Linux Kernel (5M characters). We chose $k = 20$ for the continuous HMM based on a PCA analysis of the LSTM states, as the first 20 components captured almost all the variance.

Table 1 shows the predictive log likelihood of the next text character for each method. On all text data sets, the hybrid algorithm performs a bit better than the standalone LSTM with the same number of LSTM states. This effect gets smaller as we increase the LSTM size and the HMM makes less difference to the prediction (though it can still make a difference in terms of interpretability). The hybrid algorithm with 20 HMM states does better than the one with 10 HMM states. The joint hybrid algorithm performs worse than an LSTM of the same size and is also quite slow (the SGD-based HMM may be more error-prone and slower to train than the FFBS-based HMM).

We interpret the HMM and LSTM states in the hybrid algorithm with 10 LSTM states and 10 HMM states in Figures 3 and 4, showing which features are identified by the HMM and LSTM components of the hybrid algorithm. In Figures 3a and 3c, we color-code the training data with the 10 HMM states. In Figures 3b and 3d, we apply k-means clustering to the 10 LSTM hidden states, and color-code the training data with the k-means clusters. The HMM and LSTM states pick up on spaces, indentation, and special characters in the data (such as comment symbols in Linux data). We see some examples where the HMM and LSTM complement each other, such as learning different things about spaces and comments on Linux data, or punctuation on the Shakespeare data. In Figure 2, we see that some individual LSTM hidden states identify similar features, such as comment symbols in the Linux data.

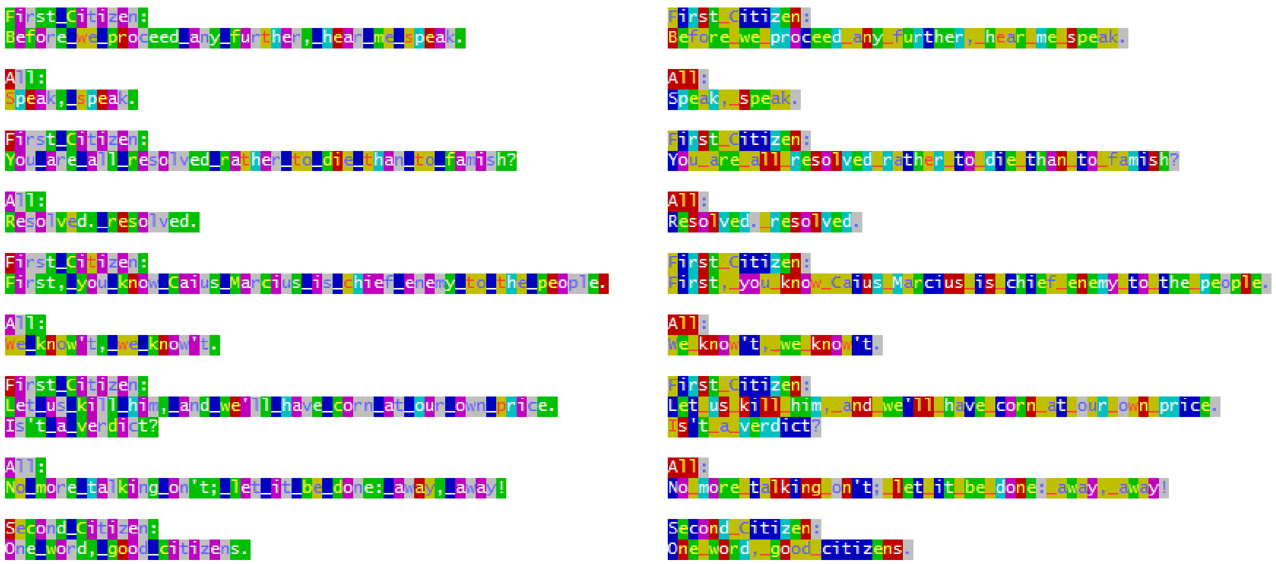

(a) Hybrid HMM states on Shakespeare data (colors correspond to 10 HMM states). Blue cluster identifies spaces. Green cluster (with white font) identifies punctuation and ends of words. Purple cluster picks up on some vowels.

(b) Hybrid LSTM states on Shakespeare data (colors correspond to 10 k-means clusters). Yellow cluster (with red font) identifies spaces. Grey cluster identifies punctuation (except commas). Purple cluster finds some 'y' and 'o' letters.

Figure 3: Visualizing HMM and LSTM states on Shakespeare data for the hybrid algorithm with 10 LSTM states and 10 HMM states. The HMM and LSTM components learn some complementary features in the text: while both learn to identify spaces, the LSTM does not completely identify punctuation or pick up on vowels, which the HMM has already done.

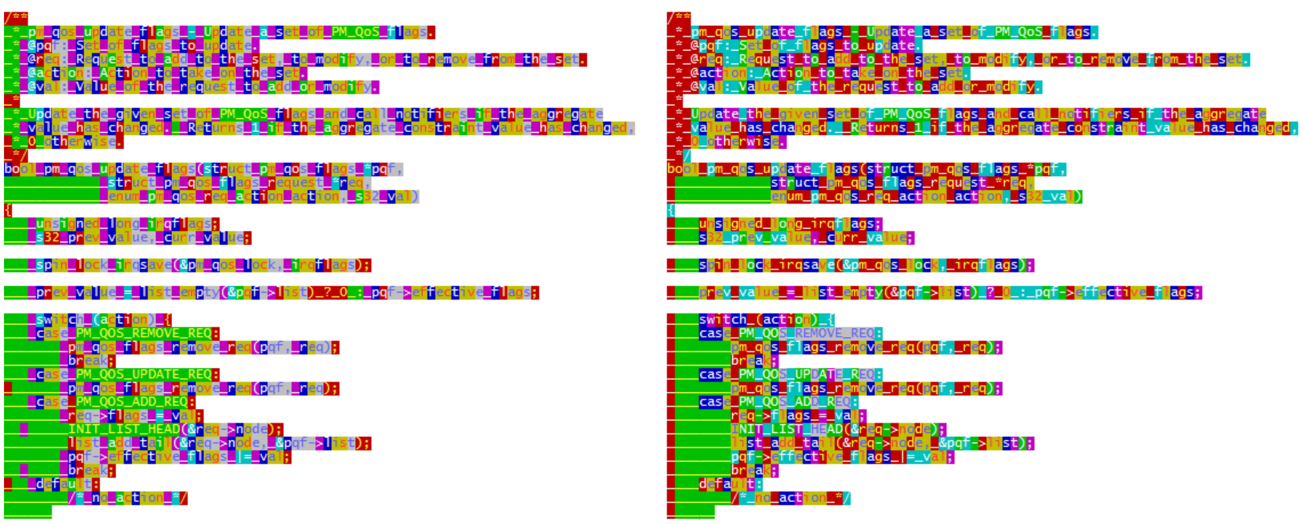

(c) Hybrid HMM states on Linux data (colors correspond to 10 HMM states). Distinguishes comments and indentation spaces (green with yellow font) from other spaces (purple). Red cluster (with yellow font) identifies punctuation and brackets. Green cluster (yellow font) also finds capitalized variable names.

(d) Hybrid LSTM states on Linux data (colors correspond to 10 K-means clusters). Distinguishes comments, spaces at beginnings of lines, and spaces between words (red with white font) from indentation spaces (green with yellow font). Opening brackets are red (yellow font) and closing brackets are green (white font).

Figure 4: Visualizing HMM and LSTM states on Linux data for the hybrid algorithm with 10 LSTM states and 10 HMM states. The HMM and LSTM components learn some complementary features in the text related to spaces and comments.

Table 1: Predictive loglikelihood comparison on the text data sets (sorted by validation set performance).

Data	Method	Parameters	LSTM states	HMM states	Validation	Training
Penn Tree Bank	HMM (cont)	1000	100	20	-2.58	-2.58
	HMM (disc)	500		10	-2.43	-2.43
	HMM (disc)	1000		20	-2.28	-2.28
	LSTM	715	5		-2.22	-2.22
	Hybrid	1715	5	10	-2.14	-2.15
	Hybrid	1715	5	20	-2.06	-2.07
	Hybrid (joint)	2830	10	10	-2.05	-2.05
	LSTM	1830	10		-1.99	-1.99
	Hybrid	2330	10	10	-1.94	-1.95
	Hybrid	2830	10	20	-1.93	-1.94
	LSTM	3345	15		-1.82	-1.83
	Hybrid	3845	15	10	-1.81	-1.82
	Hybrid	4345	15	20	-1.8	-1.81
	Hybrid (joint)	6260	20	10	-1.78	-1.79
	LSTM	5260	20		-1.72	-1.73
	Hybrid	5760	20	10	-1.72	-1.72
	Hybrid	6260	20	20	-1.71	-1.71
Shakespeare	Hybrid (joint)	3430	10	10	-3.02	-3.01
	HMM (cont)	1300		20	-2.74	-2.75
	HMM (disc)	650		10	-2.69	-2.68
	Discrete HMM	1300		20	-2.5	-2.49
	Hybrid (joint)	7160	20	10	-2.42	-2.41
	LSTM	865	5		-2.41	-2.35
	Hybrid	1515	5	10	-2.3	-2.26
	Hybrid	2165	5	20	-2.26	-2.18
	LSTM	2130	10		-2.23	-2.12
	Hybrid	2780	10	10	-2.19	-2.08
	Hybrid	3430	10	20	-2.16	-2.04
	Hybrid	4445	15	10	-2.13	-1.95
	LSTM	3795	15		-2.1	-1.95
	Hybrid	5095	15	20	-2.07	-1.92
	Hybrid	6510	20	10	-2.05	-1.87
	LSTM	5860	20		-2.03	-1.83
	Hybrid	7160	20	20	-2.02	-1.85
Linux Kernel	HMM (disc)	1000		10	-2.76	-2.7
	HMM (cont)	2000		20	-2.74	-2.75
	HMM (disc)	2000		20	-2.55	-2.5
	LSTM	1215	5		-2.54	-2.48
	Hybrid	3215	5	10	-2.33	-2.26
	Hybrid	3215	5	20	-2.25	-2.16
	Hybrid (joint)	4830	10	10	-2.22	-2.14
	LSTM	2830	10		-2.17	-2.07
	Hybrid	3830	10	10	-2.14	-2.05
	Hybrid	4830	10	20	-2.07	-1.97
	LSTM	4845	15		-2.03	-1.9
	Hybrid	5845	15	10	-1.96	-1.84
	Hybrid (joint)	9260	20	10	-1.96	-1.84
	Hybrid	6845	15	20	-1.96	-1.83
	LSTM	7260	20		-1.88	-1.73
	Hybrid	8260	20	10	-1.87	-1.73
	Hybrid	9260	20	20	-1.85	-1.71

4. Conclusion and future work

Hybrid HMM-RNN approaches combine the interpretability of HMMs with the predictive power of RNNs. Sometimes, a small hybrid model can perform better than a standalone LSTM of the same size. We use visualizations to show how the LSTM and HMM components of the hybrid algorithm complement each other in terms of features learned in the data.

References

Bourlard, Herve and Morgan, Nelson. *Connectionist speech recognition: a hybrid approach*, volume 247 of *Kluwer international series in engineering and computer science*. Kluwer Academic Publishers, Boston, 1994.

Che, Zhengping, Purushotham, Sanjay, and Liu, Yan. Distilling Knowledge from Deep Networks with Applications to Healthcare Domain. *Neural Information Processing Systems Workshop on Machine Learning for Healthcare (MLHC)*, 2015.

Karpathy, Andrej, Johnson, Justin, and Li, Fei-Fei. Visualizing and Understanding Recurrent Networks. *International Conference for Learning Representations Workshop Track*, 2016.

Kim, Been, Shah, Julie A., and Doshi-Velez, Finale. Mind the gap: A generative approach to interpretable feature selection and extraction. In Cortes, Corinna, Lawrence, Neil D., Lee, Daniel D., Sugiyama, Masashi, and Garnett, Roman (eds.), *Neural Information Processing Systems (NIPS)*, pp. 2260–2268, 2015.

Maas, A., Le, Q., O'Neil, T., Vinyals, O., Nguyen, P., and Ng, A. Recurrent Neural Networks for Noise Reduction in Robust ASR. In *Proceedings of INTERSPEECH*, 2012.

Nguyen, Anh Mai, Yosinski, Jason, and Clune, Jeff. Deep neural networks are easily fooled: High confidence predictions for unrecognizable images. In *IEEE Conference on Computer Vision and Pattern Recognition, CVPR 2015, Boston, MA, USA, June 7-12, 2015*, pp. 427–436, 2015.

Rao, Vinayak and Teh, Yee Whye. Fast MCMC sampling for Markov jump processes and extensions. *Journal of Machine Learning Research*, 14:3207–3232, 2013. arXiv:1208.4818.

Rüping, Stefan. *Learning interpretable models*. PhD thesis, Dortmund University of Technology, 2006.